Notes on Corona-Resistant Antennas for High-Voltage Sensing Applications

Prof. Gregory D. Durgin, Marcin Morys

August 13, 2018

1 Introduction

Within emerging *smart grid* technologies, there is a gaping hole in scientific knowledge regarding design, modeling, and characterization of radio antennas in high-voltage environments. Specifically, useful quantitative models do not exist for describing the dynamic physics of high-voltage AC *corona plasmas* and their influence on radiating structures; as a result, little guidance is available for the design and measurement of communication antennas that resist this phenomenon.

It has long been understood that high-voltages produce severe compatibility and noise issues for radio communications [Juh08]. Only recently, however, has the effect of *corona shielding* been measured and shown to impair UHF and microwave communication devices that operate at high-voltage line potentials [Val10]. Valenta, et. al. measured a 10 dB drop in the 5.8 GHz received power from an antenna operating at 100 kV line-to-ground AC potential [Val10]. This drop in received power was due to the surrounding corona plasma, an invisible Faraday cage that reflects and attenuates radio signals as well as de-tunes and distorts the antenna that it encapsulates. Antenna designs that resist this corona shielding are critical for wireless sensors that monitor and protect the national power grid.

2 Review of High-Voltage Corona

In this section, we review the basic physics of AC corona plasmas and preliminary results on their influence on radio communications using line-potential antennas.

2.1 Plasma Effects on Communications

The influence of plasmas on radio communications has been extensively studied for ionospheric propagation. Appleton's experiments quantified how the cold, sparse plasma of the upper atmosphere can reflect terrestrial radio waves back to the surface of the earth [App32]. Murray's experiments demonstrated how this plasma in the presence of a magnetic field leads to Faraday rotation of electromagnetic waves [Mur54]. More closely related to the corona shielding problem, Rybak showed that a spacecraft re-entering the earth's atmosphere generates hot plasmas on its exterior, shielding antennas from communications [Ryb70]. Many researchers have investigated antenna types that

resist the electrical distortions and attenuations of thermal plasmas in the context of spacecraft re-entry [Bac65].

High-voltage corona plasmas differ significantly. The alternating current on power equipment subjects high-voltage antennas to a dynamic exchange between both positive and negative corona formations. The physics describing these processes is much more complicated than the slowly varying ionosphere or re-entry plasmas. The atmospheric density of molecules on the surface of the earth also leads to very different conditions than those in space; an immediate consequence is that the high collision frequency of air at 1.0 atm leads to considerable loss per unit distance traveled by a radio wave through high-density plasma.

2.2 Positive Corona Formation

Positive corona refers to the ion formation and charge distribution processes associated with *positive* high-voltage applied to a conductor. The physical processes of positive corona formation are depicted on the left side of Figure 1. Formation of positive corona begins as electrically neutral air molecules (usually diatomic oxygen or nitrogen) absorb a sufficient quantum of energy that dissociates one of their electrons (a); this energy may be taken from incoming ionizing radiation or from the strong electric field immediately surrounding the conductor, which rips away the negative electron from the molecule, turning it into a positive ion. The low-mass electron quickly accelerates towards the conductor, while the more massive positive ion slowly accelerates away from the conductor. Further ionization occurs when some of these energetic electrons collide with neutral air molecules en route to the conductor, dissociating additional electrons (b). Although impeded by collisions, the electrons quickly reach the electro-positive conductor (c), where they freely enter.

Once this positive coronating process begins, the formation and build-up of positive ions in the vicinity of the conductor alters the nearby electric field distribution. By Gauss's law, the electro-positive ions suppress the electric field close to the conductor and intensify the field at a distance away from the conductor. Thus, the ionization process now takes place further away from the conductor (d). The massive positive ions continue to migrate away from the electropositive conductor (e) as an equilibrium is established. Eventually, the peak electric field moves far enough away from the conductor and diminishes in amplitude to establish a bounded region of corona formation. Beyond this region, the electric field is not strong enough to ionize air molecules. The region around the conductor achieves a steady-state distribution of charge and current density.

2.3 Negative Corona Formation

Negative corona refers to the ion formation and charge distribution processes associated with *negative* high-voltage applied to a conductor. The physical processes of positive corona formation are depicted on the right side of Figure 1. Negative corona begins formation in a manner similar to positive corona: non-ionizing radiation or the powerful electric field about the electro-negative conductor begins to ionize neutral atmospheric molecules (a). Further ionization occurs when high-velocity electrons, now traveling *away* from the conductor, strike other neutral molecules with enough kinetic energy to dissociate additional electrons (b).

The electrons quickly accelerate and evacuate from the immediate area of the negative conductor (c). Some may exit the region by bonding with a neutral air molecule, creating a slower-moving negative ion (d). The positive ions slowly migrate toward the electro-negative conductor (e), crowding out the neutral air molecules. Now the electric field *immediately* around the conductor intensifies,

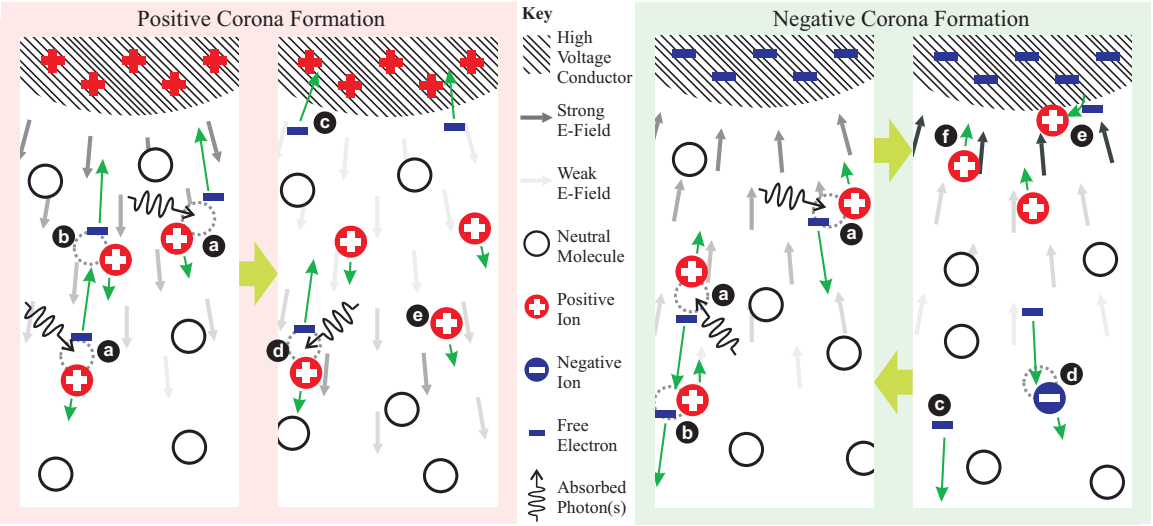

Figure 1 Illustration of the physical processes of positive (left) and negative (right) corona formation for a high-voltage conductor in air above a ground plane. Each frame illustrates a close-up view of a metallic conductor surface that sits at distance to a ground plane.

while the field at a distance diminishes in amplitude – the opposite of the positive corona case. This new field distribution provides a form of negative feedback that suspends the ionization process. This suspension is only temporary, since the positive ions, upon reaching the conductor, may pick up a free electron from the metallic surface (f). Once enough positive ions have neutralized their charge in this manner, the field distribution relaxes to its previous state and ionization begins again. Thus, negative corona does not achieve a steady state for its charge and current distribution like positive corona – *even under DC excitation*. Rather, the states of negative corona oscillate on the order of 1-100 microseconds [Loe39], [Mor97].

Even at peak ion formation, the charge distribution of negative electrons around a conductor is quite different for negative vs. positive corona. In positive corona, a monotonically increasing density of negative electrons is observed right up to the surface of the conductor [Loe39]. In negative corona, the average electron density also increases towards the surface of the conductor, but drops off significantly before the surface is reached [Che03]. These two different charge distributions lead to asymmetrical corona effects on antenna performance.

2.4 High-Voltage AC Corona Processes

Ultimately, a high-voltage AC corona consists of periodic surges of positive and negative corona formation. Although coronating mechanisms operate on a short time scale of microseconds, AC corona structure around a conductor at a given instant is not equivalent to the DC corona excited with an identical voltage level. First, the presence of residual ions affects corona formation, making it more difficult to suspend corona formation on the falling edge of a high-voltage AC waveform [Loe39]. Second, there is a range of transitional voltages that result in undulating, localized bursts of corona along a high-voltage conductor. Furthermore, corona formation can be affected by humidity,

particulate matter, wind, and precipitation [Cla07]. Finally, the potentially strong magnetic field surrounding the conductor due to various levels of AC line current also affects the corona structure [Ses73].

Although definitive models do not exist, an estimate of how corona formation and charge forms around a conductor is shown in Figure 2. For the positive half of the sinusoidal voltage on a high-voltage conductor, positive corona begins formation after a certain threshold voltage is passed. The peak electron distribution around the conductor is achieved at or shortly after the line voltage peak. The positive corona process ceases after another threshold is reached, leading to a transition period with little charge present around the conductor. During the negative half of the AC voltage excitation, the oscillatory negative corona processes commence and increase in magnitude. Again, a transition period ensues where the electron density peak around the conductor reaches a minimum. Complicating this process is the presence of current-induced magnetic fields that alter the electron and ion migration patterns near high-voltage lines. Thus, Figure 2 sketches only the qualitative behavior due to the unknown complexity and behavior of modeling dynamic corona.

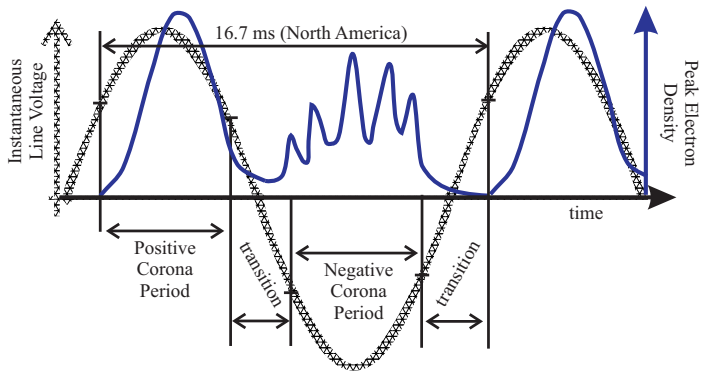

Figure 2 Illustration of the peak electron voltage over time on an AC high-voltage line. Peak electron density rises and falls in alternating cycles of positive and negative corona formation. *Charge interstices* exist both between positive and negative corona formation as well as (possibly) during intervals of negative corona formation.

3 Preliminary Investigation of Anti-Corona Antennas

The attenuation of an electromagnetic plane wave propagating through a homogeneous layer of plasma can be determined from the complex permittivity and is shown in Fig 3. For the case of the 2.4 or 5.8 GHz ISM communication bands, the attenuation is on the order of $20dB/cm$ for an electron density of $10^{20}m^{-3}$, which is a typical charge density for a badly coronating high voltage structure. Although valid specifically for TEM wave propagation rather than near fields, Fig 3 illustrates the electron densities that significantly impact radiation. Electron densities greater than $10^{19}m^{-3}$ seriously degrade the communications channel for an antenna in a plasma.

Simulations of 5.8 GHz planar patch antennas under coronating conditions illustrate their degradation in a communications link. In order to simulate a worst-case scenario for electromagnetic wave attenuation, a corona plasma that covers the entire face of the antenna substrate is simulated in HFS™. This is an idealized distribution, since much of corona formation occurs at localized points and edges rather than surfaces. The electron density in the plasma is taken to be exponentially decreasing in a series of 10 layers, with a peak value specified as 10^{18}, 10^{19}, or $10^{20}m^{-3}$. For a positive corona, the peak electron density is taken to be at the surface of the antenna, while for the negative corona, the peak electron density is set at the second layer, leaving a lower electron density adjacent to the antenna. These conditions arise from the corona formation mechanisms described

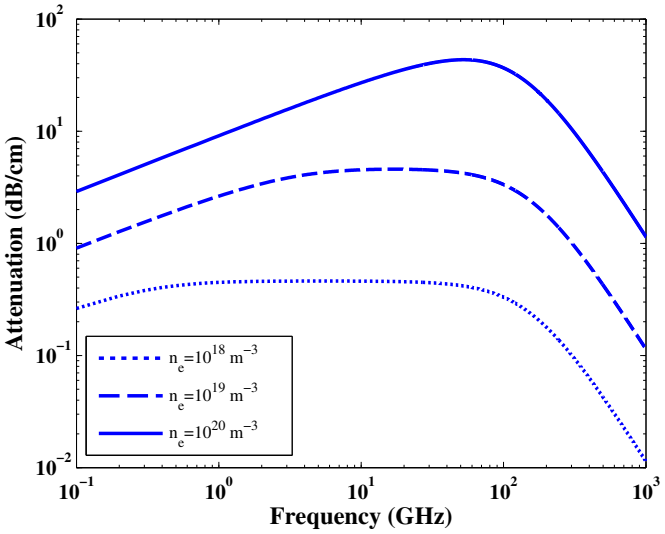

Figure 3 Attenuation of an electromagnetic wave by a plasma volume vs. wave frequency. A drude model is used with $\varepsilon_\infty = 1$ and $\nu = 10^{12} Hz$. The electron number density, n_e, dependence is shown for three typical values for a corona plasma.

Figure 4 Depiction of the model of a negative corona with a peak electron density of $n_{e,max} = 10^{19}m^{-3}$. For a negative corona, the electrons at the antenna surface have not attained sufficient energy to initiate an electron avalanche, leading to a low initial electron density. Electron density drops by an order of magnitude for each of the slabs after the peak.

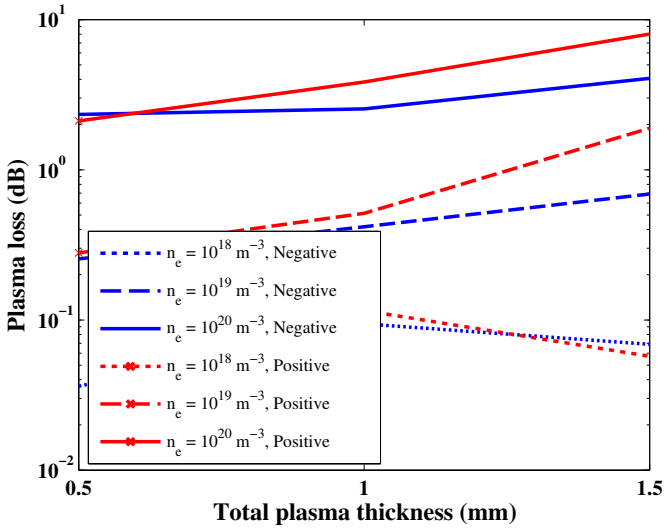

Figure 5 Loss in radiated power due to attenuation by a corona plasma formation (positive or negative) on a narrowband rectangular patch antenna.

in the previous section. The setup for the antenna simulations is shown in Fig 4.

The results for the simulations of the plasma on a rectangular patch antenna and a wideband E-shaped patch antenna are shown in Figures 5-8.

Comparing the plasma attenuation at 5.8GHz from Figure 3 with the loss incurred by a plasma covering a patch antenna in Figures 5, 7, it is observed that loss is in the same order of magnitude. There is not a significant difference between the loss due to plasma attenuation for the narrowband patch and wideband E-shaped patch antennas (within $1dB$). While the sharp resonance of the narrowband rectangular patch antenna gives it a very low reflection loss at none to low plasma densities, at higher plasma densities around $10^{20}m^{-3}$ the impedance mismatch and reflection loss increase significantly. On the other hand, the wideband E-patch antenna has a weaker resonance in free space, but it also undergoes a smaller impedance shift with a plasma present. The highest density positive corona incurs a $2dB$ higher reflection loss in the narrowband rectangular patch than in the wideband E-shaped patch antenna.

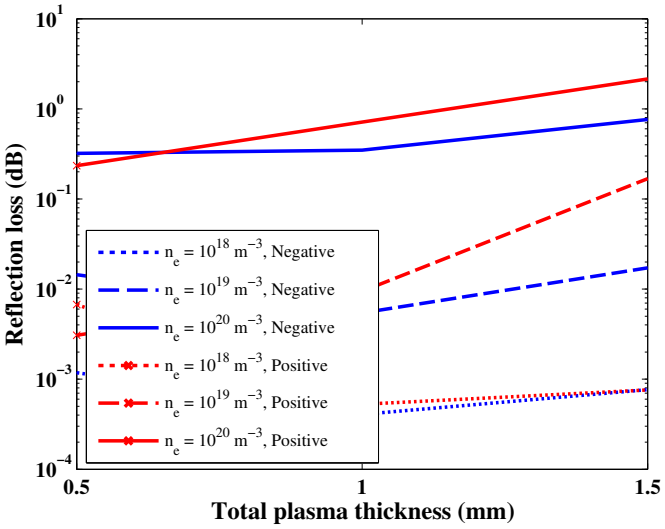

Figure 6 Loss in radiated power due to a reflection at the input port with a corona plasma formation (positive or negative) on a narrowband rectangular patch antenna.

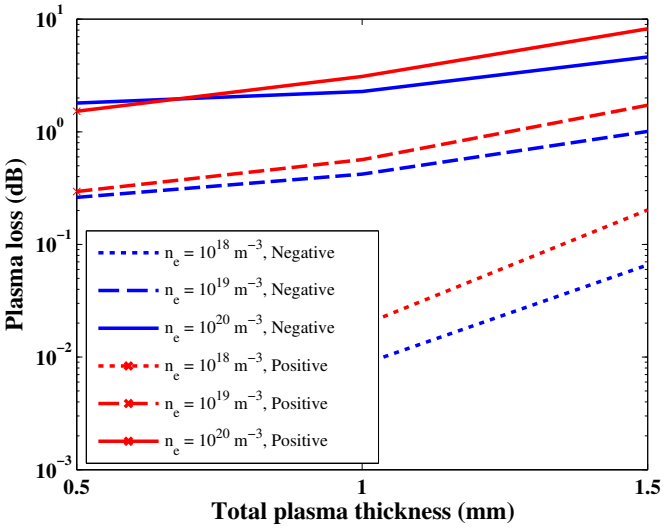

Figure 7 Loss in radiated power due to attenuation by a corona plasma formation (positive or negative) on a wideband E-shaped patch antenna.

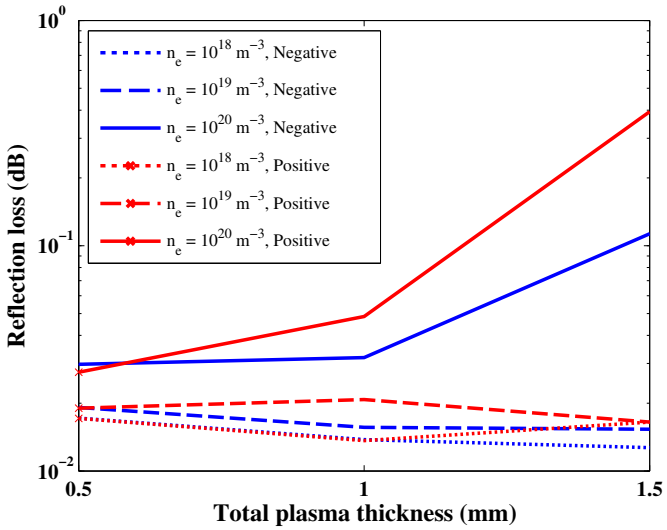

Figure 8 Loss in radiated power due to a reflection at the input port with a corona plasma formation (positive or negative) on a wideband E-shaped patch antenna.

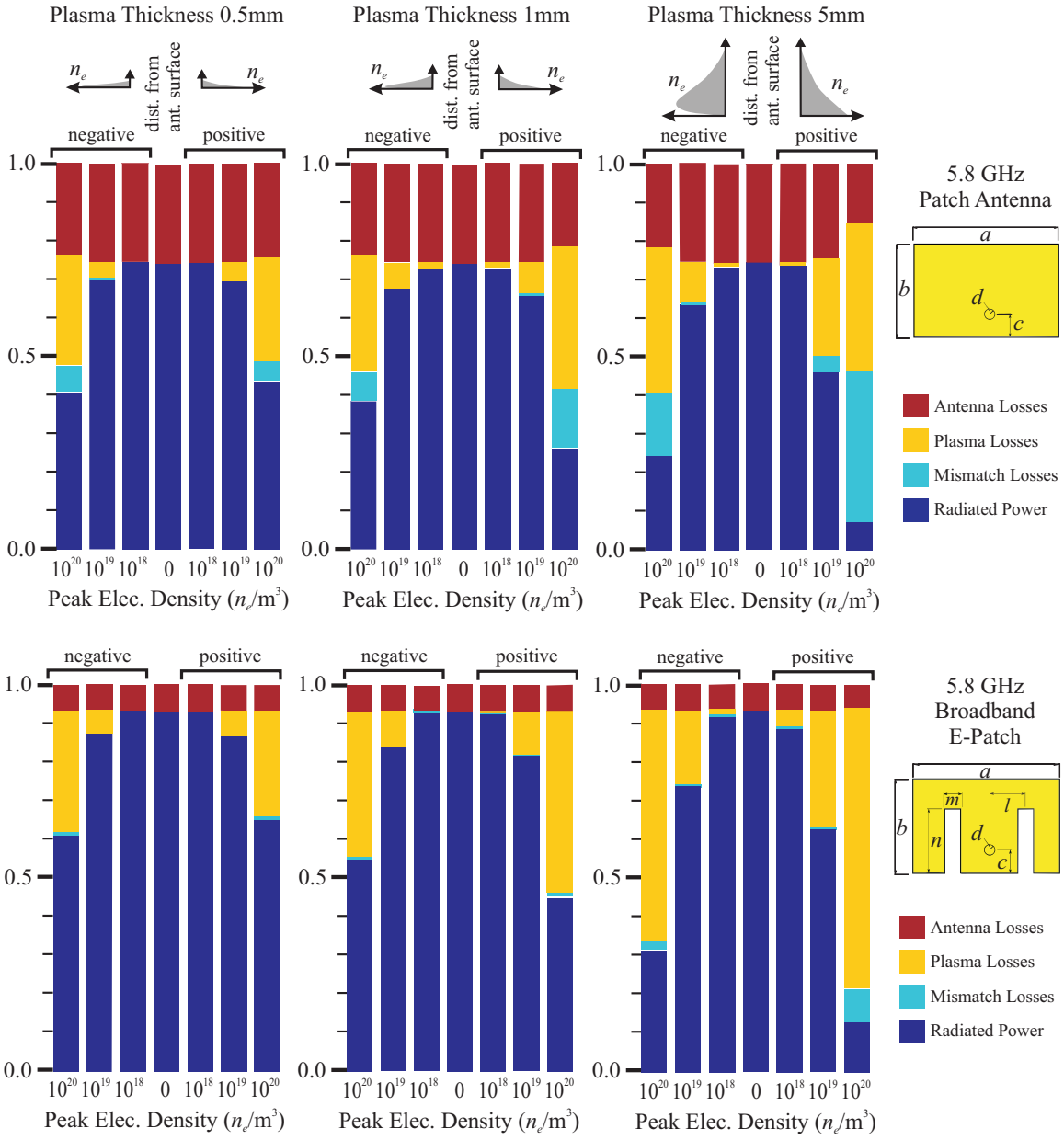

Figure 9 Summary of positive and negative corona influences on a narrowband patch and broadband-E antenna radiation by Morys. As the plasma thickness increases and the peak charge density rises, the antennas lose additional power to impedance mismatches and propagation through the charged medium.

4 Strategies for Enhancing Antenna Operation in Corona

A basic understanding of corona formation and influence on antennas leads to many possible design strategies for antennas and radios in the high-voltage environment. Consider the following approaches:

- *Field-Minimizing Antenna Manifolds:* In all designs, one must minimize the field strength immediately around the antenna, which often involves removing protrusions, sharp corners, and bends in both dielectric and metal. This strategy, by itself, is not sufficient since field stresses in precipitation or in the more compact substation environment can cause plasmas to form around a structure that is otherwise corona-free at a designed free-space voltage [New68], [Cha12], [Min10].

- *Resonance-Shifted Antenna:* As demonstrated in the previous section, the onset of plasma formation often enlarges the effective conductive surface a narrowband antenna, with link losses dominated by impedance mismatches rather than plasma attenuation. One design method is to accept this down-shifting of antenna resonance by intentionally shrinking the size of the antenna and introducing a tolerable amount of free-space mismatch loss. At the onset of corona formation, the resonance will shift back into the desired band, removing mismatch losses just as the plasma-induced medium losses increase.

- *Broadband Antenna:* Certain types of broadband antennas resist the plasma-induced impedance mismatch losses experienced by narrowband antennas. As Figure 9 demonstrates, a simple 3 dB gain is possible from switching the antenna topology from a narrowband square patch structure to a wider-band E-shaped patch structure.

- *High-Magnetic Field Antenna:* Preliminary results also suggest that the field distributions immediately around the antenna may influence the plasma medium losses. Lower current densities on the radiating structure and the reduced magnetic fields may change the near-field medium loss.

- *Charge Interstitial Transmission:* In addition to the antenna itself, it is also possible to modify the wireless communications protocol to take advantage of low-levels of charge distribution that occurs periodically in an AC high-voltage system (see Figure 2). Through simple field sensing, the high-voltage communications device can modify modulation or delay packet transmission to minimize the path loss experienced in the wireless link.

Bibliography

[App32] Edward V. Appleton, "Wireless studies of the ionosphere," *Wireless Section, Institution of Electrical Engineers-Proceedings of the*, vol. **7**, no. 21, pp. 257–265, 1932.

[Bac65] M.P. Bachynski, "Electromagnetic wave penetration of reentry plasma sheaths," *Radio Science Journal of Research*, vol. **69D**, no. 2, pp. 147–154, 1965.

[Cha12] Sreenita Chatterjee, "Design of corona control rings for EHV/UHV line hardwares and substations," in *Properties and Applications of Dielectric Materials (ICPADM), 2012 IEEE 10th International Conference on the*, 2012, pp. 1–4.

[Che03] J. Chen and J. H Davidson, "Model of the negative dc corona plasma: comparison to the positive dc corona plasma," *Plasma chemistry and plasma processing*, vol. **23**, no. 1, pp. 83–102, 2003.

[Cla07] J. J. Clade, C. H. Gary, and C. A. Lefevre, "Calculation of corona losses beyond the critical gradient in alternating voltage," *Power Apparatus and Systems, IEEE Transactions on*, , no. 5Part-I, pp. 695–703, 2007.

[Dur09] G. D Durgin, C. Valenta, P. Graf, M. Trotter, G. Koo, and B. Schafer, "5.8 GHz backscatter sensor measurement across high voltage insulation gaps," Tech. Rep., Georgia Institute of Technology, Atlanta, GA, Apr. 2009.

[Juh08] L.-E. Juhlin, J. Skansen, L. Koppari, E. Petersson, and P. Stenumgaard, "Measurement of radio frequency interference from high voltage substations backgrounds and considerations for future emission requirements," Paris, France, 2008.

[Loe39] Leonard B. Loeb, *Fundamental Processes of Electrical Discharge In Gasses*, John Wiley & Sons, Inc., New York, 1939.

[Min10] Xu Mingming, Li Kejun, Tan Zhenyu, and Niu Lin, "Study on tubular busbar corona design optimization of +-660kV HVDC converter substation in qingdao," June 2010, pp. 5663–5666, IEEE.

[Mor97] R. Morrow, "The Theory of Positive Glow Corona," *Journal of Physics D: Applied Physics*, vol. **30**, pp. 3099–3114, 1997.

[Mur54] W.A.S. Murray and J.K. Hargreaves, "Lunar radio echoes and the faraday effect in the ionosphere," *Nature*, vol. **173**, no. 4411, pp. 944–945, 1954.

[New68] HOBART H. Newell, Tseng-Wu Liao, and F. W. Warburton, "Corona and RI caused by particles on or near EHV conductors: II-Foul weather," *Power Apparatus and Systems, IEEE Transactions on*, , no. 4, pp. 911–927, 1968.

[Ryb70] J.P. Rybak, "Causes, effects and diagnostic measurements of the reentry plasma sheath," Tech. Rep. AD718428, Colorado State University, 1970.

[Ses73] S.R. Seshadri, *Fundamentals of Plasma Physics*, American Elsevier Publishing Company, Inc., New York, 1973.

[Val10] C. R Valenta, P. A Graf, M. S Trotter, G. A Koo, G. D Durgin, and B. J Schafer, "Backscatter channel measurements at 5.8 GHz across high-voltage corona," Hilo, HI, Nov. 2010.